



NACA

# RESEARCH MEMORANDUM

INFLUENCE OF TUBE-ENTRANCE CONFIGURATION ON AVERAGE  
HEAT-TRANSFER COEFFICIENTS AND FRICTION FACTORS FOR

AIR FLOWING IN AN INCONEL TUBE

By Warren H. Lowdermilk and Milton D. Grele

Lewis Flight Propulsion Laboratory  
Cleveland, Ohio

TECHNICAL REPORT  
AFMDC  
1-52 2817-107

NATIONAL ADVISORY COMMITTEE  
FOR AERONAUTICS

WASHINGTON  
August 23, 1950

319.98/13



NACA RM E50E23

## NATIONAL ADVISORY COMMITTEE FOR AERONAUTICS

RESEARCH MEMORANDUM

INFLUENCE OF TUBE-ENTRANCE CONFIGURATION ON AVERAGE HEAT-TRANSFER  
COEFFICIENTS AND FRICTION FACTORS FOR AIR FLOWING IN AN  
INCONEL TUBE

By Warren H. Lowdermilk and Milton D. Grele

## SUMMARY

A heat-transfer investigation, which is an extension of two previously reported NACA investigations, was conducted with air flowing through an electrically heated Inconel tube having an inside diameter of 0.402 inch, a length of 24 inches, and having either a long-approach or a right-angle-edge entrance. The range of conditions included Reynolds numbers from 1000 to 375,000, average inside-tube-wall temperatures from 660° to 2000° R, and heat-flux densities up to 120,000 Btu per hour per square foot.

The conventional method of correlating heat-transfer data wherein properties of air were evaluated at the average bulk temperature resulted in a decrease in heat-transfer parameter for an increase in inside-tube-wall temperature at constant Reynolds number. Good correlation of the heat-transfer data for the entire range of temperatures investigated was obtained when the Reynolds number was modified by substituting the product of air density evaluated at the average inside-tube-wall temperature and the velocity evaluated at the average bulk temperature for the conventional mass flow per unit cross-sectional area. The other physical properties of the air were evaluated at the inside-tube-wall temperature. These findings substantiate the work previously done.

The conventional method of plotting friction factors, calculated from a dynamic pressure based on an average air density against Reynolds number, resulted in a considerable spread of the data with temperature level. A fair correlation of the friction data was obtained when the friction factors were calculated from a dynamic pressure based on a film density and plotted against the modified surface Reynolds number.

Changing the entrance section had a negligible effect on the average heat-transfer coefficients and friction factors over the range of conditions investigated.

## INTRODUCTION

An experimental investigation has been instituted at the NACA Lewis laboratory to obtain surface-to-fluid heat-transfer and associated pressure-drop information over a wide range of inside-tube-wall temperatures and heat-flux densities.

As part of this general program, an investigation is being conducted with air flowing through an electrically heated Inconel tube having various entrance configurations, an inside diameter of 0.402 inch, and an effective heat-transfer length of 24 inches to obtain heat-transfer and friction data. The results of investigations conducted with a rounded entrance to this tube over ranges of Reynolds numbers from 7000 to 500,000, average inside-tube-wall temperatures from 605° to 2050° R, heat-flux densities up to 150,000 Btu per hour per square foot, and tube-exit Mach numbers up to 1.0 are reported in references 1 and 2.

In order to ascertain further the validity of the modified correlation presented in references 1 and 2 and to determine the effects of entrance configuration on over-all heat-transfer coefficients and friction factors, an investigation was conducted with two other types of entrance to the heater tube, a long-approach and a right-angle-edge section for approximately the same conditions in the turbulent range of Reynolds number as the round entrance. Results of this investigation are presented herein and are compared with those of references 1 and 2.

## APPARATUS AND PROCEDURE

The experimental setup is essentially the same as described in detail in reference 1. For convenience, however, the apparatus is briefly reviewed.

### Arrangement of Apparatus

A schematic diagram of the heater tube and associated equipment is shown in figure 1. Compressed air is supplied through a pressure-regulating valve and a cleaner to a surge tank. From the

1339 surge tank, the air flows through a second pressure-regulating valve into a preheater and then through a metering orifice and a bank of rotameters. From the rotameters the air flows into a calming tank, through the heater tube, and into a mixing tank from which it is discharged to the atmosphere.

Electric power is supplied to the heater tube from a 208-volt 60-cycle supply line through an autotransformer and a 14:1 power transformer. The low-voltage leads of the power transformer are connected to the heater-tube flanges by copper cables. The capacity of the electric equipment is 15 kilovolt-amperes.

#### Heater Tube

The Inconel tube, which is shown in figure 2, has an inside diameter of 0.402 inch and a wall thickness of 0.049 inch. Steel flanges welded to the tube at each end provide electrical contact with the transformer leads from the power supply. The tube acts as a heating element and the distance between the outer face of the steel flanges, which for this investigation is 24 inches, is taken as the effective heat-transfer length. The heater tube is thermally insulated.

Static-pressure taps are located at 11 stations along the length of the tube (fig. 2). Outside-tube-wall temperatures are measured at 30 locations by chromel-alumel thermocouples (two thermocouples located 180° apart at each of 15 stations) and a self-balancing indicating-type potentiometer.

Investigations were made with two types of heater-tube entrance, a long-approach entrance having a length of 24 inches and a right-angle-edge entrance. (See fig. 3.) Both types of entrance have an inside diameter equal to that of the heater tube (0.402 in.).

#### Range of Conditions

Heat-transfer and associated pressure-drop data were obtained with both the long-approach entrance and the right-angle-edge entrance over a range of Reynolds numbers from 1000 to 375,000, average inside-tube-wall temperatures from 660° to 2000° R, and heat-flux densities up to 120,000 Btu per hour per square foot of heat-transfer area.

## SYMBOLS

The following symbols are used in this report:

A	cross-sectional area, (sq ft)
$c_p$	specific heat of air at constant pressure, (Btu/(lb)(°F))
D	inside diameter of heater tube, (ft)
f	average friction factor
$f_b$	average bulk friction factor
$f_f$	modified film friction factor
$f_s$	modified surface friction factor
G	mass flow per unit cross-sectional area, (lb/(hr)(sq ft))
g	acceleration due to gravity, $4.17 \times 10^8$ (ft/hr <sup>2</sup> )
h	average heat-transfer coefficient, (Btu/(hr)(sq ft)(°F))
k	thermal conductivity of air, (Btu/(hr)(sq ft)(°F/ft))
L	effective heat-transfer length of heater tube, (ft)
p	static pressure, (lb/sq ft absolute)
$\Delta p$	over-all static-pressure drop across heater tube, (lb/sq ft)
$\Delta p_{fr}$	friction static-pressure drop across heater tube, (lb/sq ft)
R	gas constant for air, 53.35 (ft-lb/(lb)(°F))
S	heat-transfer area of heater tube, 0.211 (sq ft)
T	total temperature, (°R)
$T_b$	average bulk temperature equal to average of entrance and exit total temperatures, (°R)
$T_f$	average film temperature equal to half the sum of average bulk and average inside-tube-wall temperatures, (°R)
$T_s$	average inside-tube-wall temperature, (°R)

$t$	static temperature, ( $^{\circ}\text{R}$ )
$V$	velocity, (ft/hr)
$W$	air flow, (lb/hr)
$\mu$	absolute viscosity of air, (lb/(hr)(ft))
$\rho$	density of air, (lb/cu ft)
$\rho_{av}$	average density of air, (lb/cu ft)
$c_p \mu / k$	Prandtl number
$DG / \mu$	Reynolds number
$\rho_f V_b D / \mu_f$	modified film Reynolds number
$\rho_s V_b D / \mu_s$	modified surface Reynolds number
$hD / k$	Nusselt number
$h / c_{p,s} \rho_s V_b$	modified Stanton number

## Subscripts:

1	heater-tube entrance
2	heater-tube exit
b	bulk (when applied to properties, indicates evaluation at average bulk temperature)
f	film (when applied to properties, indicates evaluation at average film temperature)
s	surface (when applied to properties, indicates evaluation at average inside-tube-wall temperature)

## RESULTS AND DISCUSSION

### Heat Balance

The heat balance is shown in figure 4 where the ratio of the electric heat input minus heat loss to the heat transfer to air, as measured by weight flow and temperature rise, is plotted against the heat transfer to the air. The heat loss was found in the same manner as reported in reference 1. The heat balance is good except for some cases at low air-flow rates and corresponding low rates of heat transfer, where a decided difference was obtained between the measured values of the enthalpy increase of the air and the electric heat input minus the losses.

The air-flow and temperature-rise measurements were believed to be somewhat more dependable than the electrical measurements (particularly the heat-loss measurements) at low flow rates; therefore the heat-transfer coefficient is calculated herein from the flow rate and the temperature rise of the air.

### Correlation of Heat-Transfer Coefficients

The method of calculating the heat-transfer coefficient is the same as that given in references 1 and 2; the principal parts, however, are repeated.

The average heat-transfer coefficient  $h$  was computed from the experimental data by the relation

$$h = \frac{Wc_{p,b}(T_2 - T_1)}{S(T_s - T_b)}$$

The bulk temperature of the air  $T_b$  was taken as the arithmetic mean of the total temperatures at the entrance  $T_1$  and the exit  $T_2$  of the heater tube. The average inside-tube-wall temperature  $T_s$  was taken as an integrated average of the local outside-tube-wall temperatures minus the temperature drop through the wall.

Conventional correlation. - The average heat-transfer coefficients are plotted in the conventional manner in figure 5 for the data obtained with the long-approach entrance, where Nusselt number divided by Prandtl number raised to the 0.4 power

1339  $(hD/k_b)/(c_{p,b}\mu_b/k_b)^{0.4}$  is plotted against Reynolds number  $DG/\mu_b$ . Included for comparison is the average line (dashed) obtained by McAdams from correlation of the data of various investigations (reference 3). Also tabulated in figure 5 are the average values of  $T_s$  and  $T_s/T_b$  for the range of Reynolds numbers covered at each temperature level. The physical properties of air are based on bulk temperature. All physical properties used herein are obtained from reference 4.

A family of parallel lines having a slope of about 0.8 is obtained for the different temperature levels above a Reynolds number of about 10,000. The low-temperature data are in fair agreement with the reference line; however, as the temperature level is raised the data fall progressively below the reference line. Similar results for the round entrance were found in references 1 and 2.

The data for the right-angle-edge entrance gave similar results and are therefore not presented herein.

Correlation based on modified surface Reynolds number. - Average heat-transfer coefficients are correlated in figure 6 according to the method presented in references 1 and 2; that is, Nusselt number divided by Prandtl number to the 0.4 power is plotted against a Reynolds number that has been modified by substituting the product of density evaluated at the average inside-tube-wall temperature  $\rho_s$  and air velocity evaluated at the average bulk temperature  $V_b$  for the conventional mass flow per unit cross-sectional area  $G$ . The properties of the air appearing in the various parameters are evaluated at the average inside-tube-wall temperature  $T_s$ . Included for comparison is the curve obtained with the round-entrance data (reference 2).

The use of the modified surface Reynolds number results in a good correlation of the data over the range of conditions investigated. The data are best represented by the line previously obtained with the round entrance (reference 2).

Data for the right-angle-edge entrance in figure 7 are correlated in the same manner as in figure 6 using the modified surface Reynolds number. The curve shown is from reference 2 for the round-entrance data and from figure 6 herein for the long-approach data. The data are in good agreement with the round-entrance and long-approach data.



The data for round, long-approach, and right-angle-edge entrances for Reynolds numbers above about 10,000 can be represented by the equation

$$\frac{hD}{k_s} = 0.023 \left( \frac{\rho_s V_b D}{\mu_s} \right)^{0.8} \left( \frac{c_{p,s} \mu_s}{k_s} \right)^{0.4}$$

When the heat-transfer coefficients are computed using the electric heat input minus the heat loss rather than the heat transfer to air (as measured by weight flow and temperature rise) and are correlated in the same manner as in figure 6, the data can be represented by a single straight line down to a Reynolds number of 1000. This line is just slightly higher than the one shown in figure 6, but the data have the same relative scatter. As previously stated, however, the data using  $Wc_p(T_2 - T_1)$  is believed to be more reliable because of the uncertainty of electrical and heat-loss measurements at the low flow rates. In the turbulent range of Reynolds numbers for which the apparatus was designed, the difference in the method of evaluating heat-transfer coefficients is insignificant.

Correlation based on modified surface Reynolds number neglecting Prandtl number. - A plot of Nusselt number  $hD/k_s$  against the modified surface Reynolds number  $\rho_s V_b D / \mu_s$  for the long-approach data is given in figure 8. The properties of air in the various parameters are evaluated at the average inside-tube-wall temperature. The plot is the same as figure 6, except that the Prandtl number has been omitted. Included for comparison is the curve obtained with the round-entrance data (reference 2). The omission of Prandtl number has a negligible effect on the correlation; this effect is expected because Prandtl number varies only slightly with temperature. The right-angle-edge data, not included herein, show similar trends. The long-approach and right-angle-edge data above a modified surface Reynolds number of 10,000 can be represented by the following equation:

$$\frac{hD}{k_s} = 0.019 \left( \frac{\rho_s V_b D}{\mu_s} \right)^{0.8}$$

Correlation based on modified film Reynolds number. - The data for the long-approach entrance are replotted in figure 9 in a manner similar to that of figure 6, except that a modified film Reynolds

number is used and the air properties in the various parameters are evaluated at the average film temperature  $T_f$ . Nusselt number divided by Prandtl number to the 0.4 power  $(hD/k_f)/(c_{p,f}\mu_f/k_f)^{0.4}$  is plotted against the modified film Reynolds number  $\rho_f V_b D/\mu_f$ .

The modified film Reynolds number is obtained from the conventional Reynolds number  $DG/\mu_b$  by the relation

$$\frac{\rho_f V_b D}{\mu_f} = \left( \frac{DG}{\mu_b} \right) \left( \frac{\mu_b}{\mu_f} \right) \left( \frac{T_b}{T_f} \right)$$

Comparison of figures 6 and 9 indicates that better correlation of the data is obtained by using  $T_s$  rather than  $T_f$  in the evaluation of Reynolds number and air properties. For example, the use of  $T_f$  results in a 15-percent decrease in the Nusselt number/Prandtl number<sup>0.4</sup> for an increase in  $T_s/T_b$  from 1.19 to 2.27 as compared with no noticeable trend with the use of  $T_s$ . Similar results were obtained with the right-angle-edge entrance.

#### Correlation of Friction Factors

The method of calculating the friction factors is essentially the same as described in reference 2. The important details and the pertinent equations are, however, repeated for convenience.

Average friction factors were calculated from the experimental pressure-drop data as follows: The friction pressure drop was first obtained by subtracting the calculated momentum pressure drop from the measured drop in static pressure across the tube, thus

$$\Delta p_{fr} = \Delta p - \frac{W}{gA} (V_2 - V_1) = \Delta p - \left( \frac{W}{A} \right)^2 \frac{R}{g} \left( \frac{t_2}{p_2} - \frac{t_1}{p_1} \right)$$

An average friction factor  $f_b$  was then calculated from the friction pressure drop by the use of the conventional relation

$$f_b = \frac{\Delta p_{fr}}{\frac{L}{D} \frac{\rho_{av} V_b^2}{2g}}$$

where the average density was taken as

$$\rho_{av} = \frac{1}{R} \left( \frac{p_1 + p_2}{t_1 + t_2} \right)$$

Friction factors with no heat addition. - The average bulk half-friction factor  $f_b/2$  is plotted against the Reynolds number  $DG/\mu_b$  for the condition of no heat addition in figure 10 for both entrances. Isothermal half-friction factors for a round entrance are also shown. Included for comparison is the curve (solid) representing the Kármán-Nikuradse relation between friction factor and Reynolds number, which is

$$\frac{1}{\sqrt{8 \frac{f}{2}}} = 2 \log_{10} \left( \frac{DG}{\mu} \sqrt{8 \frac{f}{2}} \right) - 0.8$$

and the line (dashed) representing the equation for laminar flow in circular tubes, which is

$$\frac{f}{2} = \frac{8}{DG/\mu}$$

In the two foregoing equations, the values of Reynolds number and friction factor correspond to the abscissa and ordinate, respectively, in figure 10 and succeeding figures.

Good agreement with the Kármán-Nikuradse relation is obtained with all three entrance sections in the turbulent-flow range of Reynolds numbers.

Conventional correlation with heat addition. - The average bulk half-friction factor  $f_b/2$  is plotted against Reynolds number  $DG/\mu_b$  in figure 11 under conditions of heat addition with the long-approach entrance. Data for no heat addition and the Kármán-Nikuradse and laminar-flow lines are included for comparison. The data corresponding to low values of  $T_g/T_b$  agree fairly well with that for no heat addition. As  $T_g/T_b$  is increased, however,  $f_b/2$  is increased in the low Reynolds number region and

decreased in the high Reynolds number region. Similar effects were obtained with the right-angle-edge entrance, as well as the round entrance (reference 2).

Correlation based on modified surface Reynolds number. - The modified surface half-friction factor calculated from a dynamic pressure based on air density evaluated at the average inside-tube-wall temperature  $f_s/2$  is plotted against the modified surface Reynolds number  $\rho_s V_b D / \mu_s$  in figure 12 for the long-approach entrance. Data for no heat addition and the Kármán-Nikuradse and laminar-flow lines are included for comparison. The relation between  $f_s$  and  $f_b$  is

$$f_s = \frac{2T_s}{t_1 + t_2} f_b$$

The correlation results in an overcorrection of the temperature effect shown in figure 11. Similar results were obtained with the round-entrance (reference 2) and the right-angle-edge data.

Correlation based on modified surface Reynolds number and average film temperature. - The modified film half-friction factor calculated from a dynamic pressure based on air density evaluated at the average film temperature  $f_f/2$  is plotted against the modified surface Reynolds number  $\rho_s V_b D / \mu_s$  in figures 13 and 14 for the long-approach and the right-angle-edge entrances, respectively. The relation between the modified film friction factor  $f_f$  and the average bulk friction factor  $f_b$  is

$$f_f = \frac{2T_f}{t_1 + t_2} f_b$$

The isothermal data, as well as the Kármán-Nikuradse and laminar-flow lines, are included.

The data for the long-approach entrance (fig. 13) show fair agreement with the Kármán-Nikuradse line in the range of turbulent Reynolds numbers. At low Reynolds numbers, the data have about the same slope as the reference line for laminar flow, but are displaced in the direction of higher Reynolds numbers.

The correlation for the right-angle-edge data also agrees fairly well with the Kármán-Nikuradse line, as shown in figure 14. When friction factors for the round-entrance data (reference 2) are calculated from a dynamic pressure based on density at the film rather than the surface temperature, similar trends are obtained.

#### Comparison of Friction and Heat-Transfer Data

The experimental friction and heat-transfer data points for the long-approach entrance are compared in figure 15. The modified film half-friction factor  $f_f/2$  for the friction data and the product of a modified Stanton number and Prandtl number to the

$$0.6 \text{ power } \left( \frac{h}{c_{p,s} \rho_s V_b} \right) \left( \frac{c_{p,s} \mu_s}{k_s} \right)^{0.6} \text{ for the heat-transfer data}$$

are plotted against the modified surface Reynolds number  $\rho_s V_b D / \mu_s$ . The figure indicates that both the friction and heat-transfer data can be represented fairly well by a single line for modified Reynolds numbers above about 10,000. Similar results are obtained with the right-angle-edge entrance.

#### SUMMARY OF RESULTS

The results of a heat-transfer investigation conducted with air flowing through an electrically heated Inconel tube with either a long-approach or a right-angle-edge entrance, an inside diameter of 0.402 inch, and a length of 24 inches over a range of Reynolds numbers from 1000 to 375,000, average inside-tube-wall temperatures from 660° to 2000° R, and heat-flux densities up to 120,000 Btu per hour per square foot showed that:

1. The following results substantiate the findings of previous investigations with a round-entrance tube:

a. Correlation of the average heat-transfer coefficients according to the familiar Nusselt relation, wherein physical properties were evaluated at the average bulk temperature, resulted in a progressive separation of the data with increased inside-tube-wall temperature.

b. A good correlation of the heat-transfer data for the entire range of temperatures was obtained when a modified surface Reynolds number was used and the air properties were evaluated at

the inside-tube-wall temperature. The data for the long-approach, right-angle-edge, and round entrance can be represented by the same line.

c. Friction factors calculated from a dynamic pressure based on an average air density were considerably affected by temperature when plotted against Reynolds number. As the temperature level was increased, the friction factors increased in the low Reynolds number region and decreased in the high Reynolds number region.

2. A fair correlation of the friction data was obtained when the average friction factors were calculated from a dynamic pressure based on a film density and plotted against the modified surface Reynolds number.

3. A comparison indicated that both the friction data evaluated at the film temperature and the heat-transfer data evaluated at the inside-tube-wall temperature can be represented fairly well by a single line for modified surface Reynolds numbers above about 10,000.

4. The use of different entrances to the heater tube (long approach and right-angle edge) had a negligible effect on the heat-transfer and friction data, over the range of conditions investigated, when compared with results of the round-entrance data.

Lewis Flight Propulsion Laboratory,  
National Advisory Committee for Aeronautics,  
Cleveland, Ohio.

#### REFERENCES

1. Humble, Leroy V., Lowdermilk, Warren H., and Grele, Milton D.: Heat Transfer from High-Temperature Surface to Fluids. I - Preliminary Investigation with Air in Inconel Tube with Rounded Entrance, Inside Diameter of 0.4 Inch, and Length of 24 Inches. NACA RM E7L31, 1948.
2. Lowdermilk, Warren H., and Grele, Milton D.: Heat Transfer from High-Temperature Surfaces to Fluids. II - Correlation of Heat-Transfer and Friction Data for Air Flowing in Inconel Tube with Rounded Entrance. NACA RM E8L03, 1949.

3. McAdams, William H.: Heat Transmission. McGraw-Hill Book Co., Inc., 2d ed., 1942, p. 168.
4. Tribus, Myron, and Boelter, L. M. K.: An Investigation of Aircraft Heaters. II - Properties of Gases. NACA ARR, Oct. 1942.

x Thermocouples

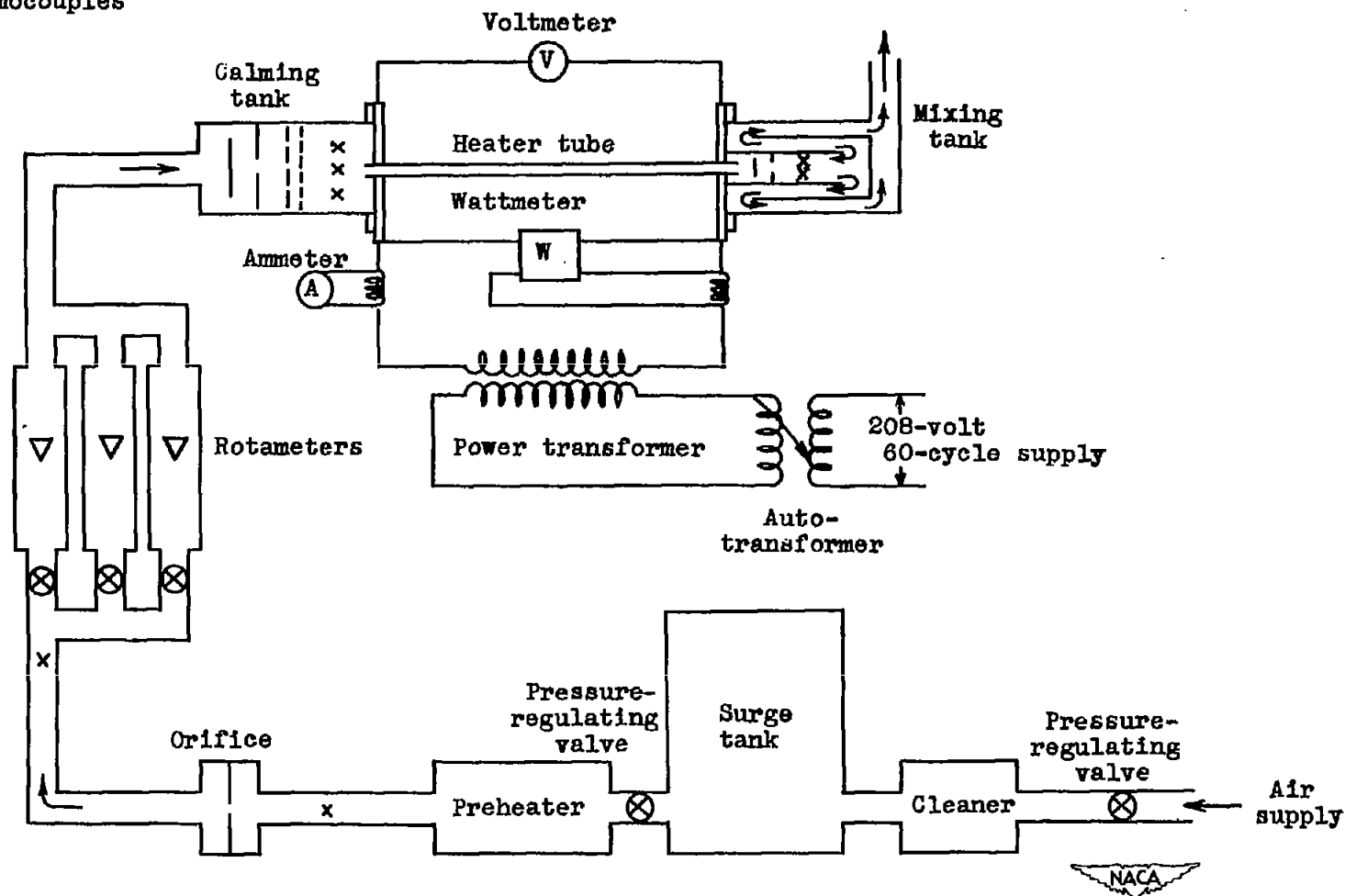


Figure 1. - Schematic diagram showing arrangement of apparatus.



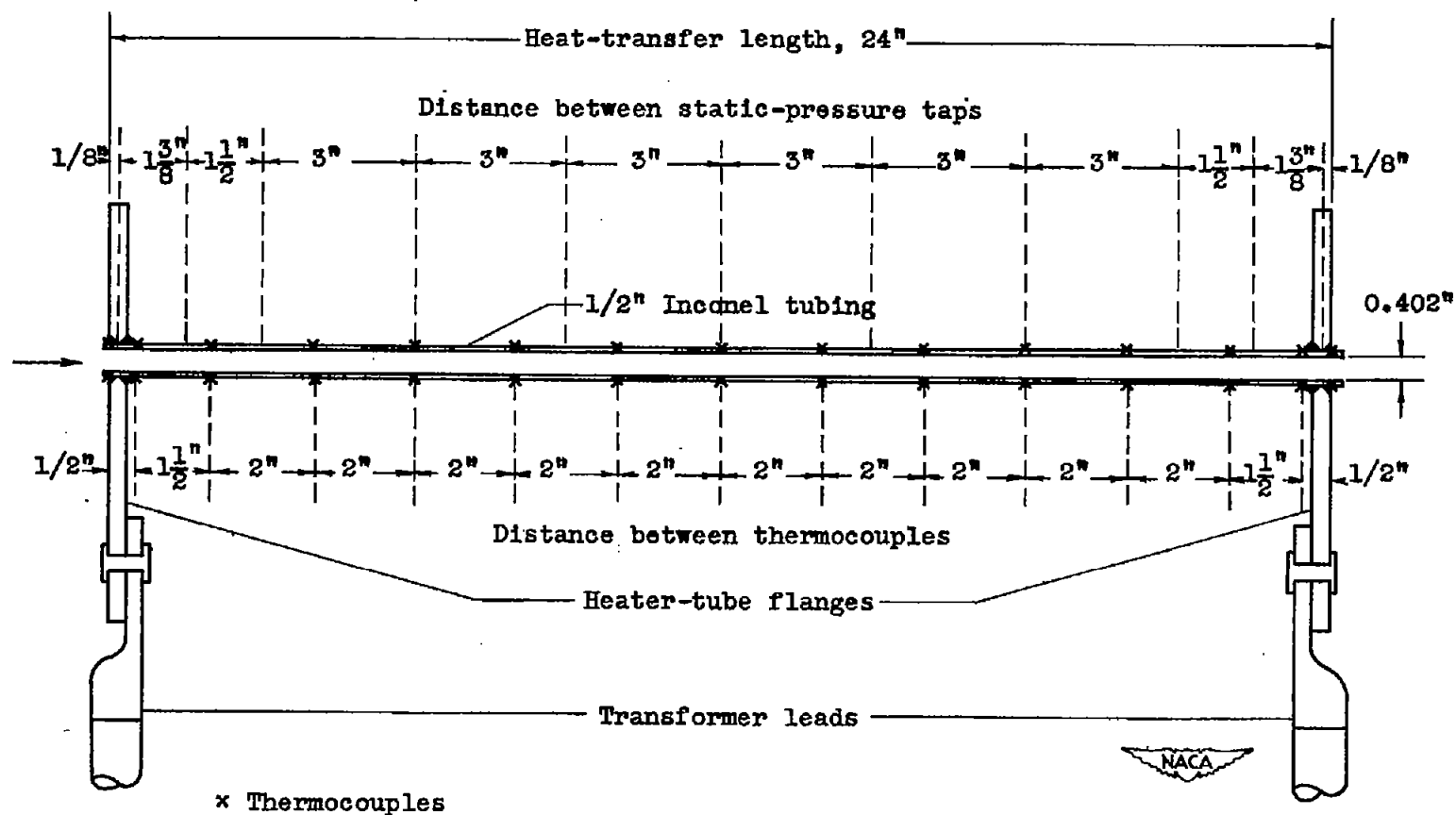


Figure 2. - Schematic diagram of heater tube showing thermocouple and pressure-tap locations.

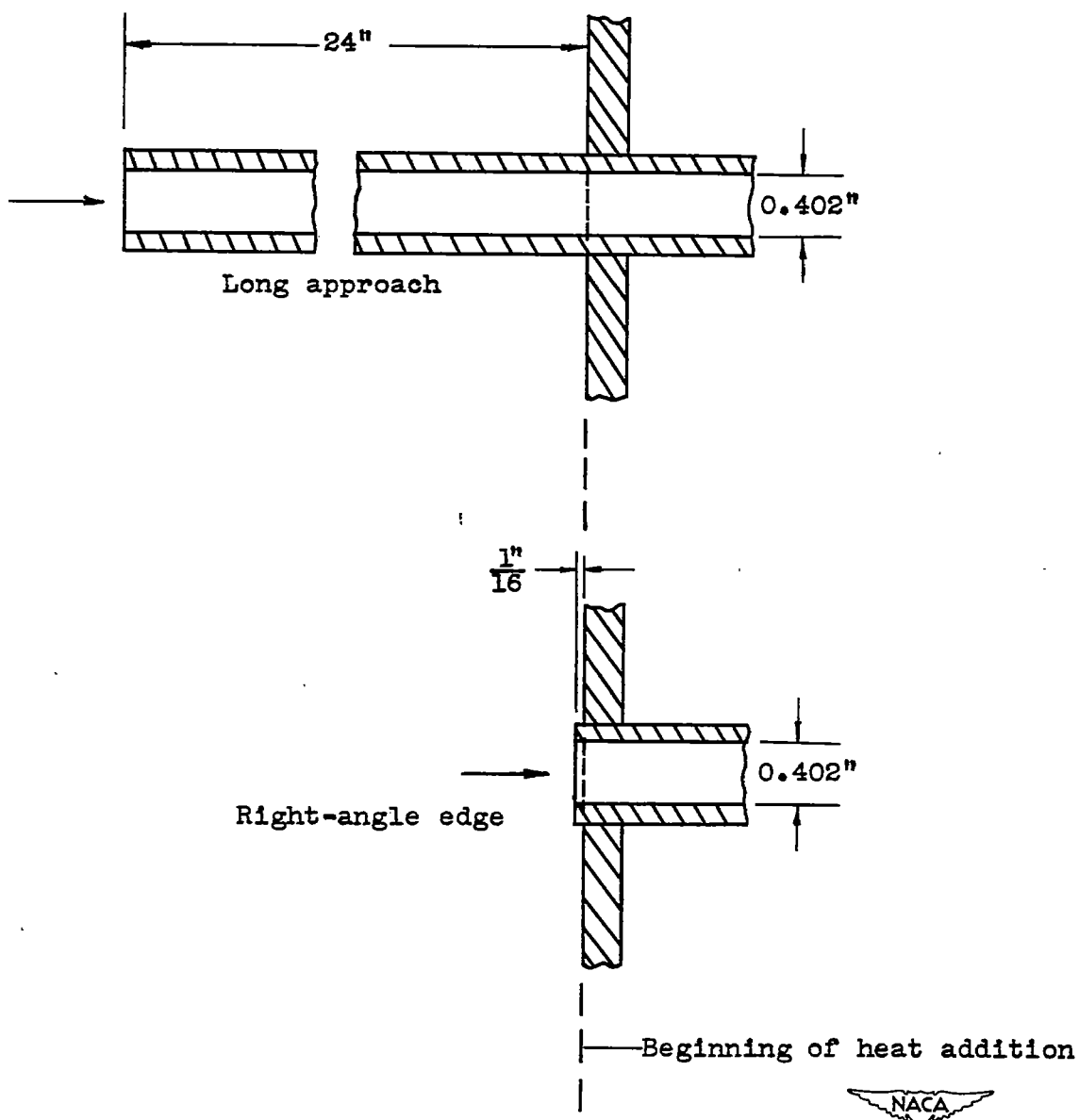
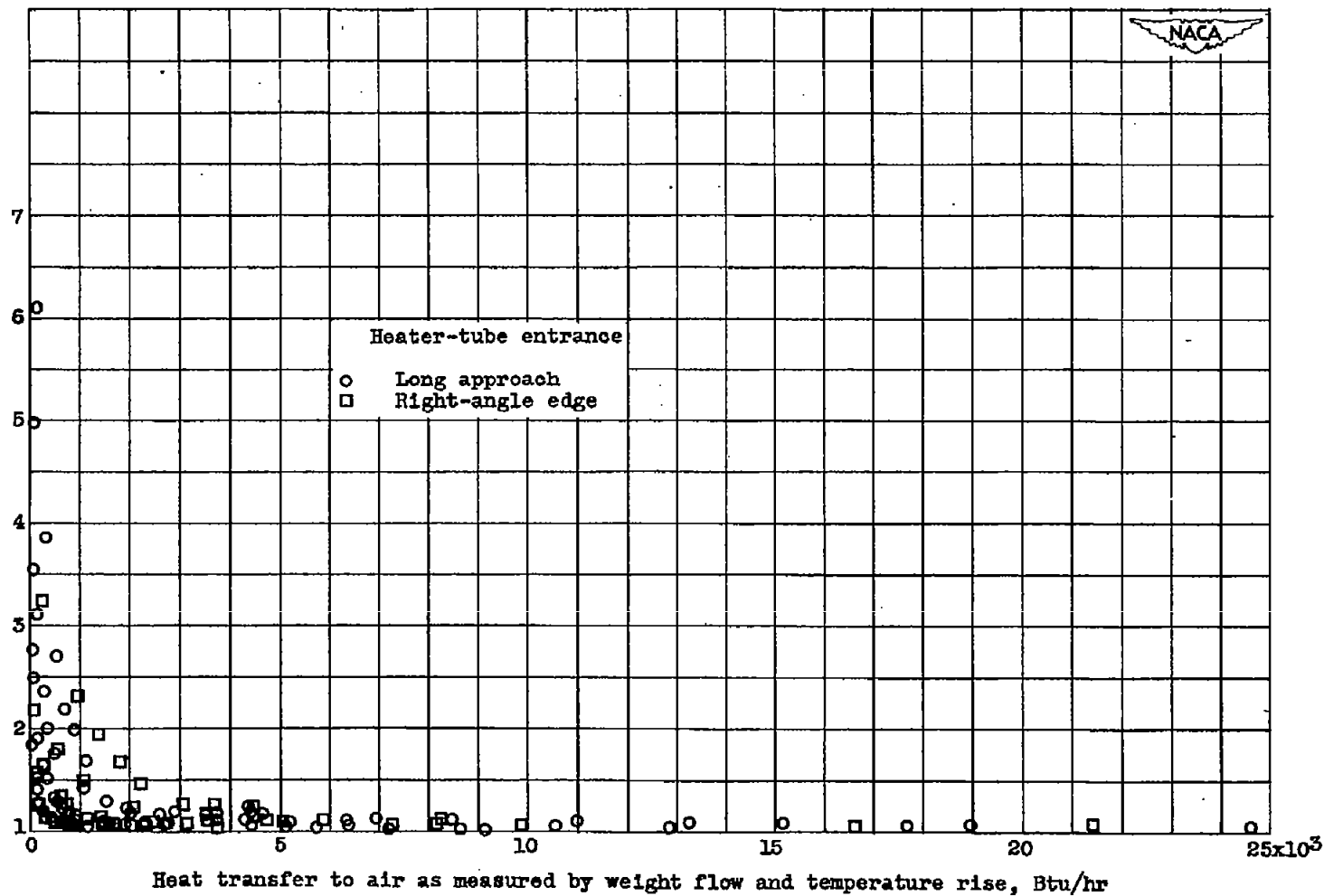


Figure 3. - Entrances to heater tube.

Electric heat input - heat loss  
Heat transfer to air as measured by weight flow and temperature rise



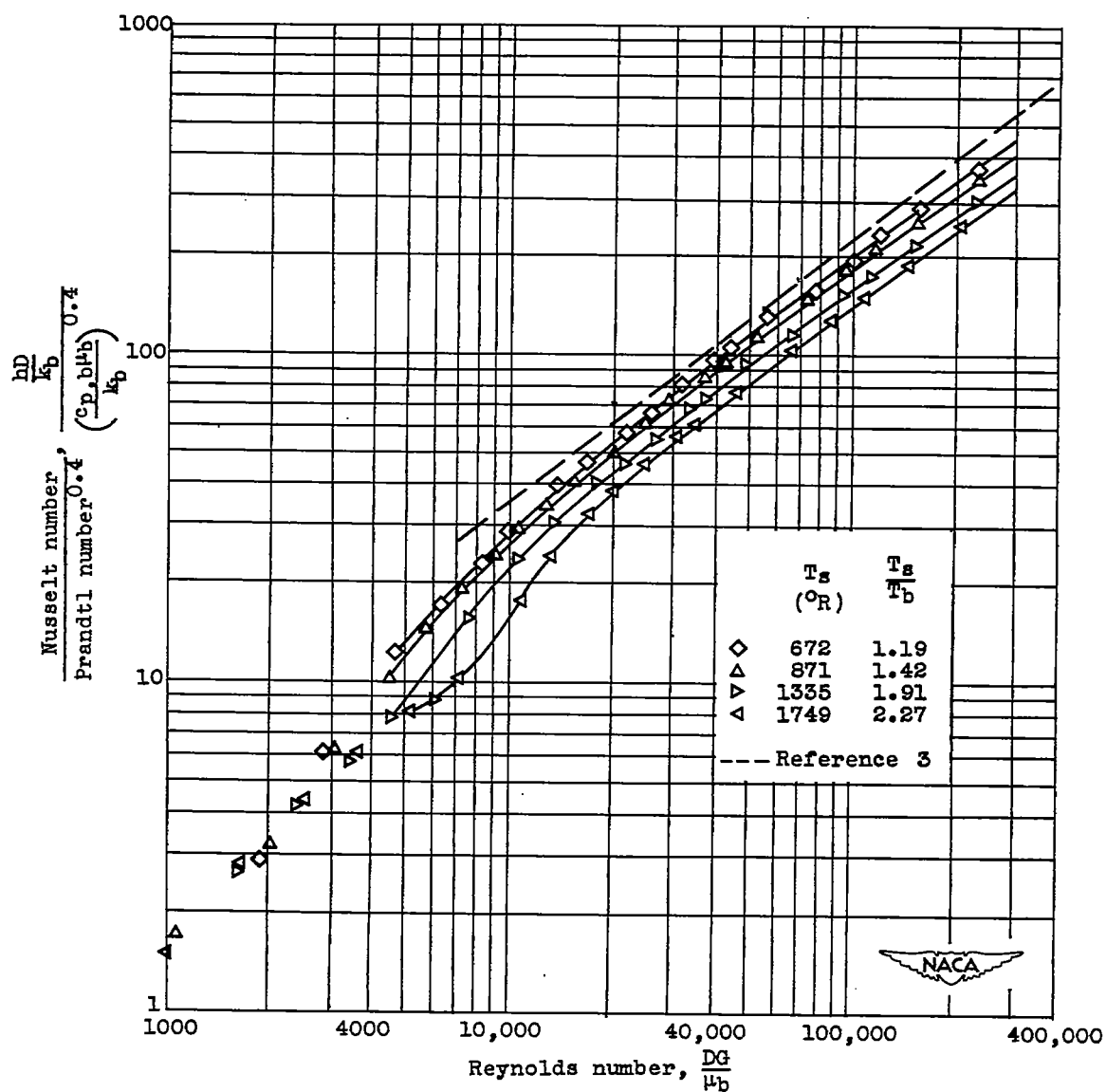


Figure 5. - Conventional correlation of heat-transfer data for long-approach entrance. Physical properties of air evaluated at  $T_b$ .

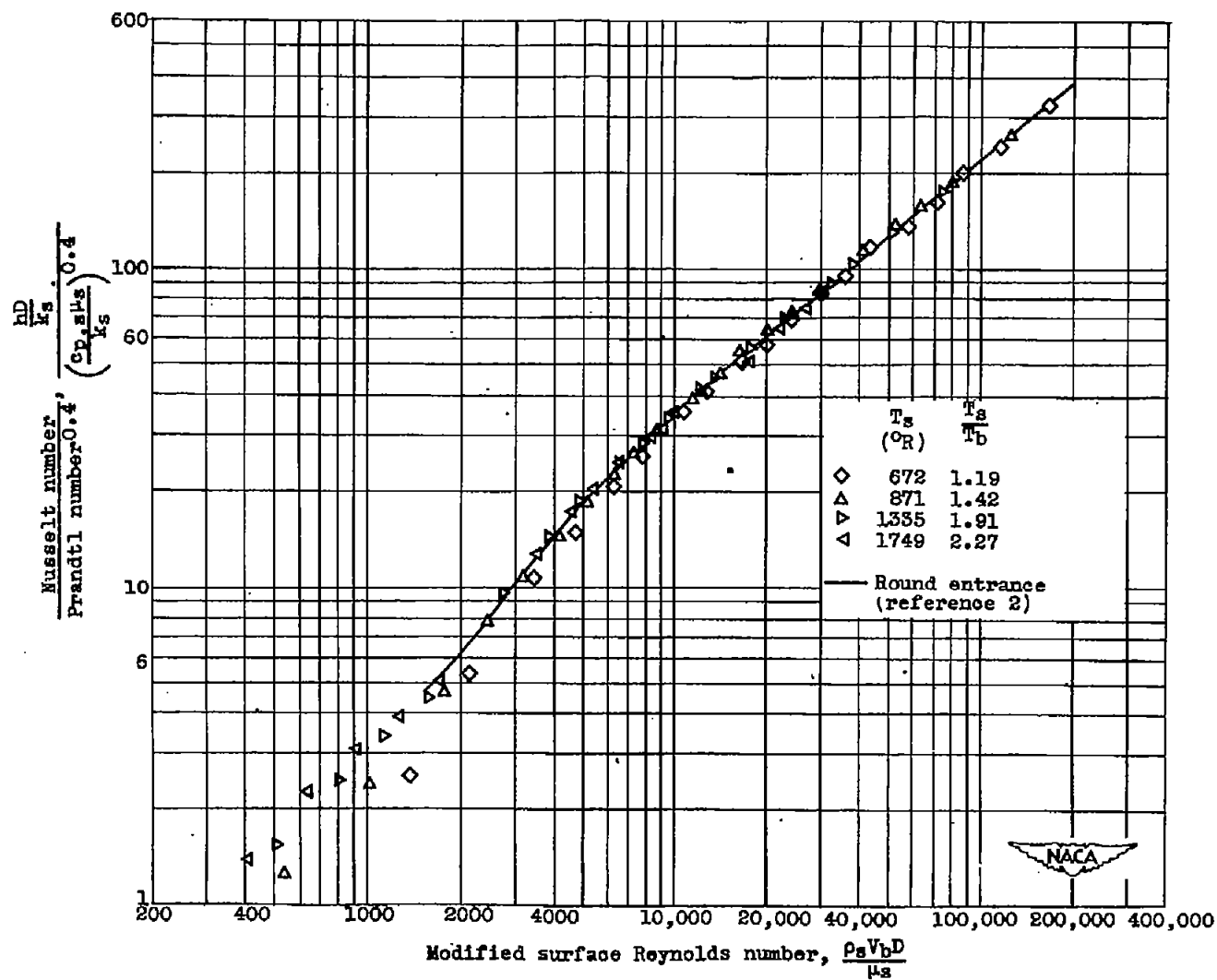


Figure 6. - Correlation of heat-transfer data for long-approach entrance using modified surface Reynolds number. Physical properties of air evaluated at  $T_s$ .

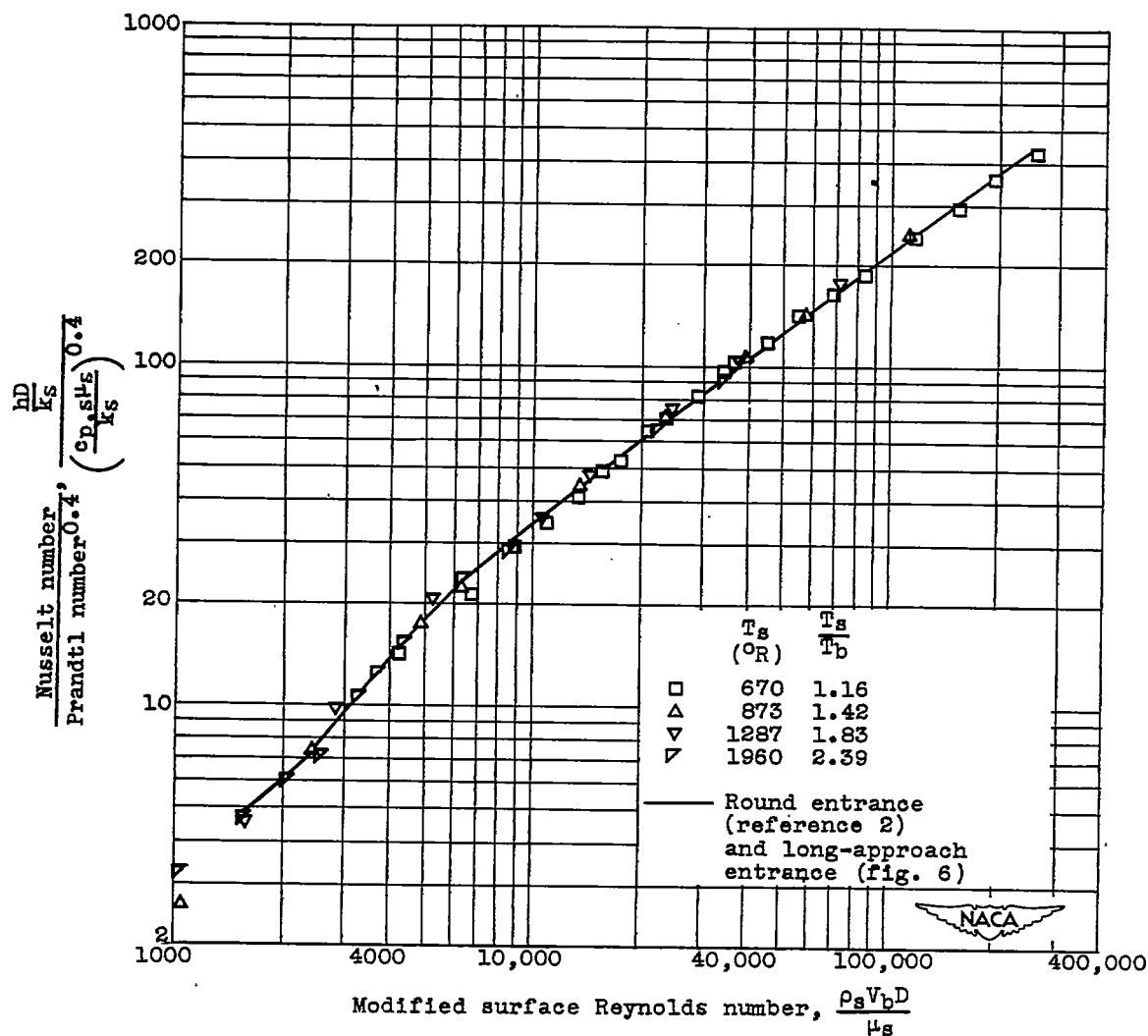


Figure 7. - Correlation of heat-transfer data for right-angle-edge entrance using modified surface Reynolds number. Physical properties of air evaluated at  $T_s$ .

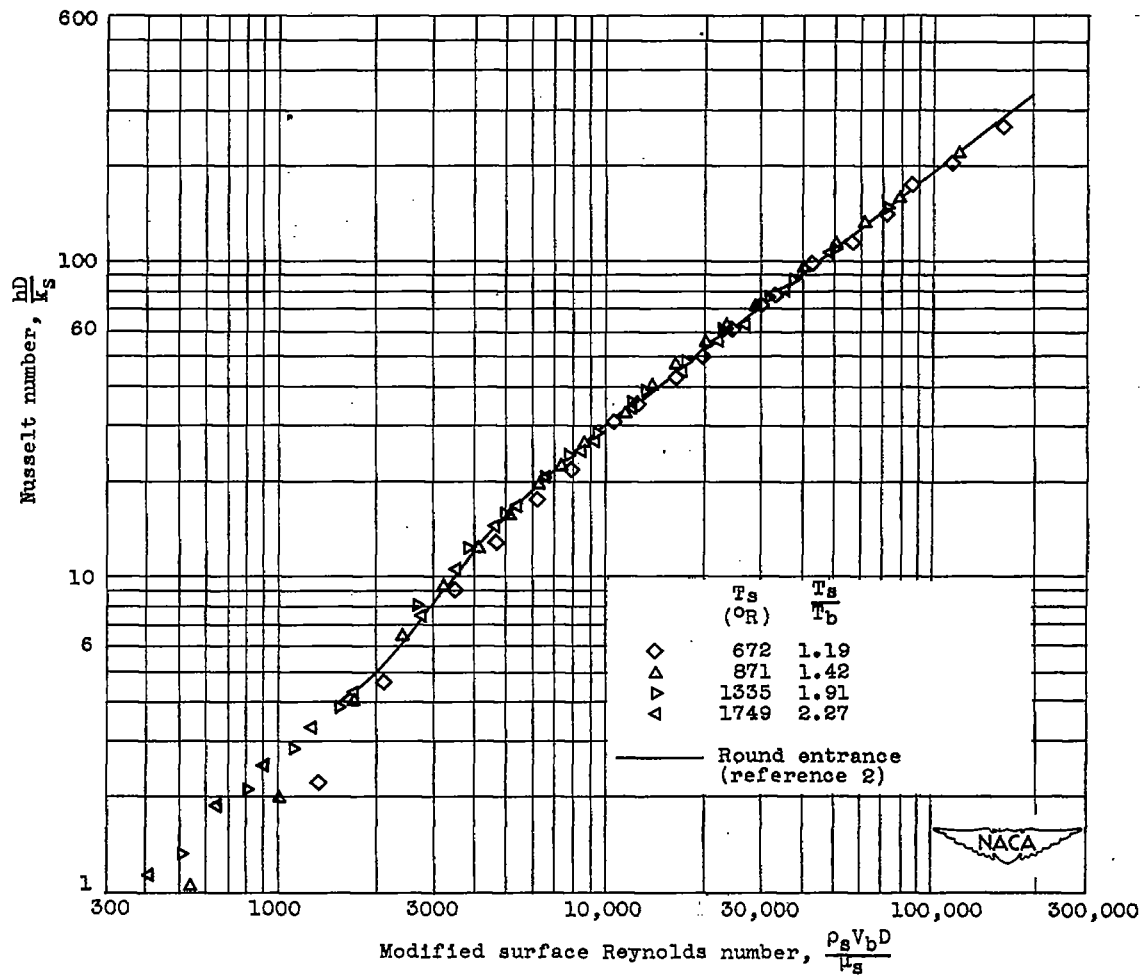


Figure 8. - Correlation of heat-transfer data for long-approach entrance using modified surface Reynolds number and neglecting Prandtl number. Physical properties of air evaluated at  $T_s$ .

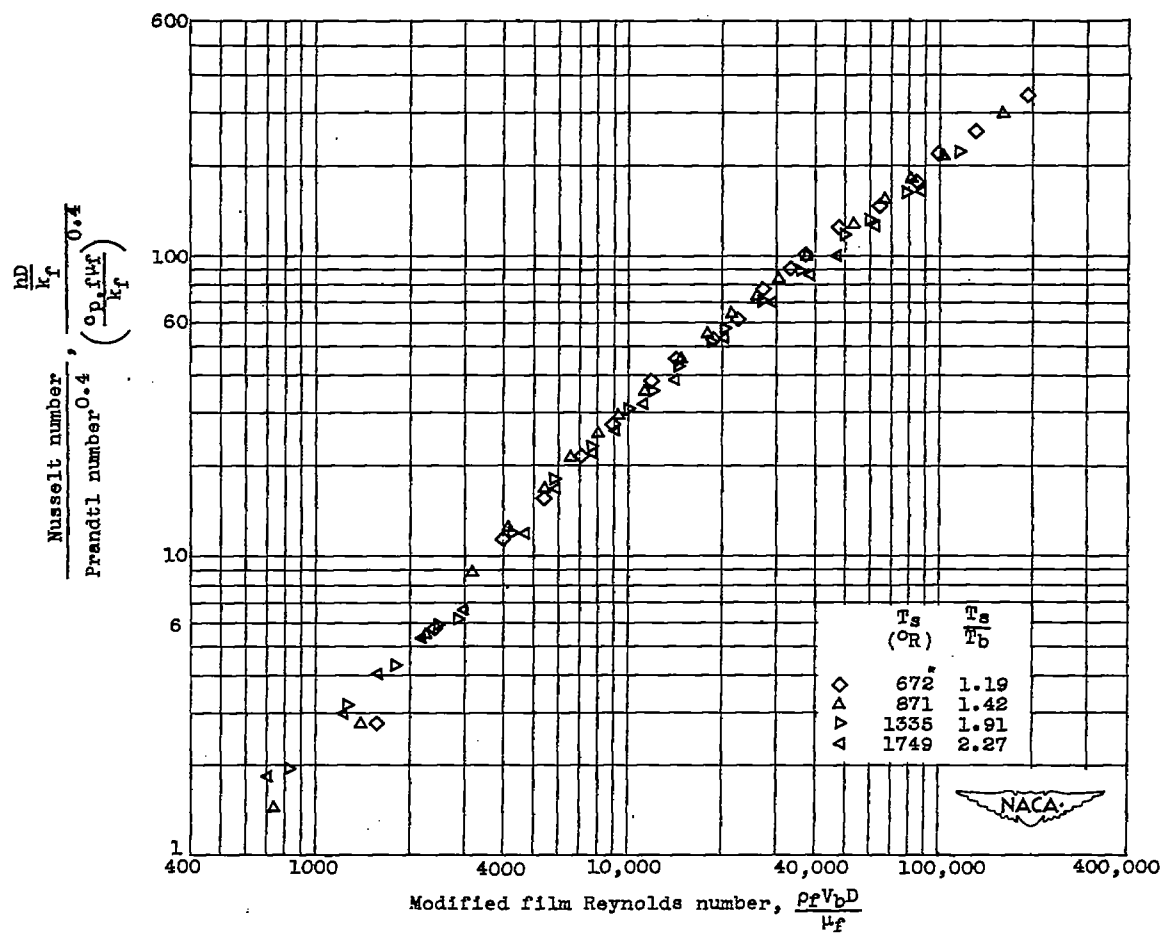


Figure 9. - Correlation of heat-transfer data for long-approach entrance using modified film Reynolds number. Physical properties of air evaluated at  $T_f$ .



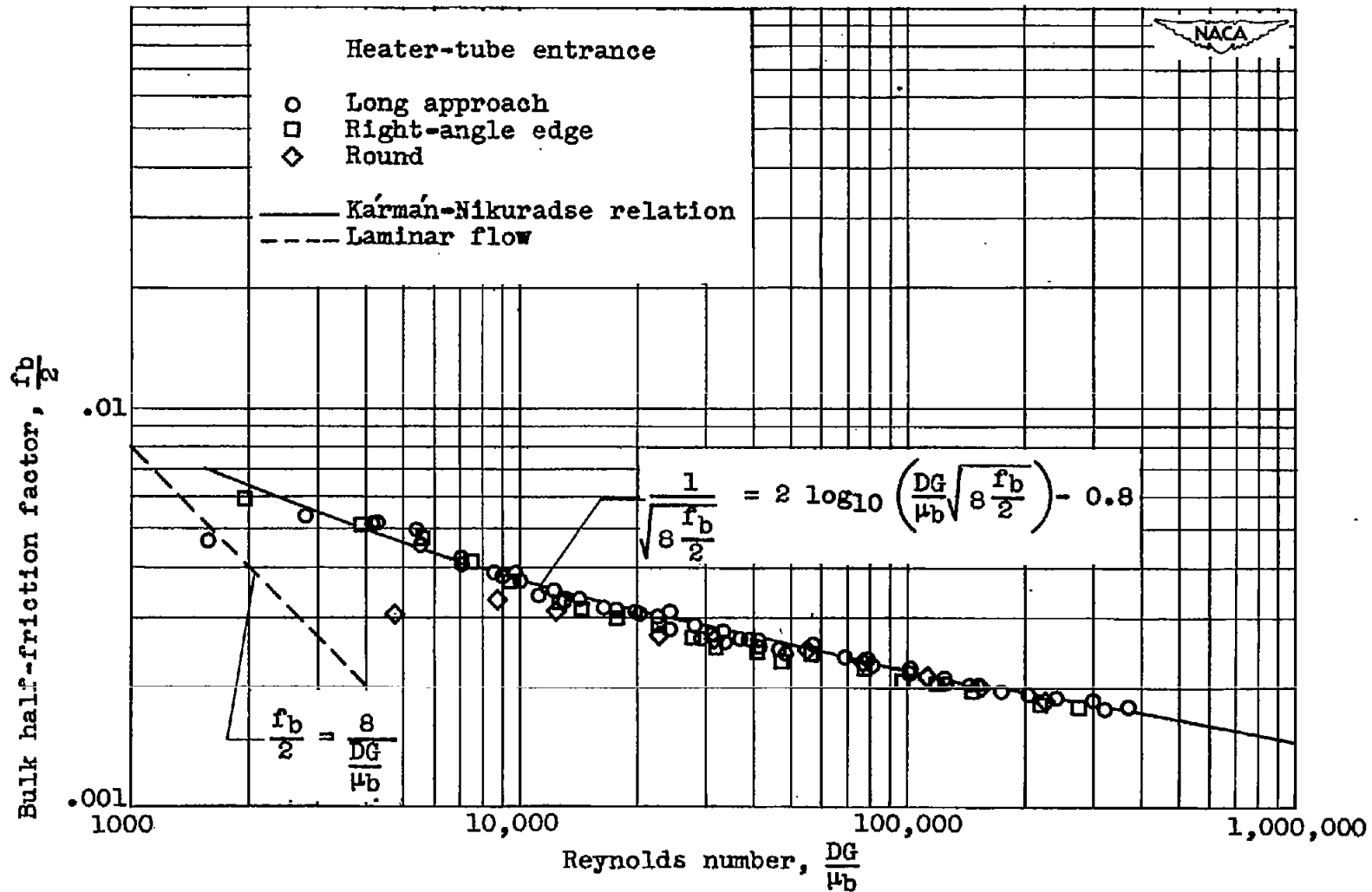


Figure 10. - Variation of bulk half-friction factor with Reynolds number with no heat addition for all entrances.

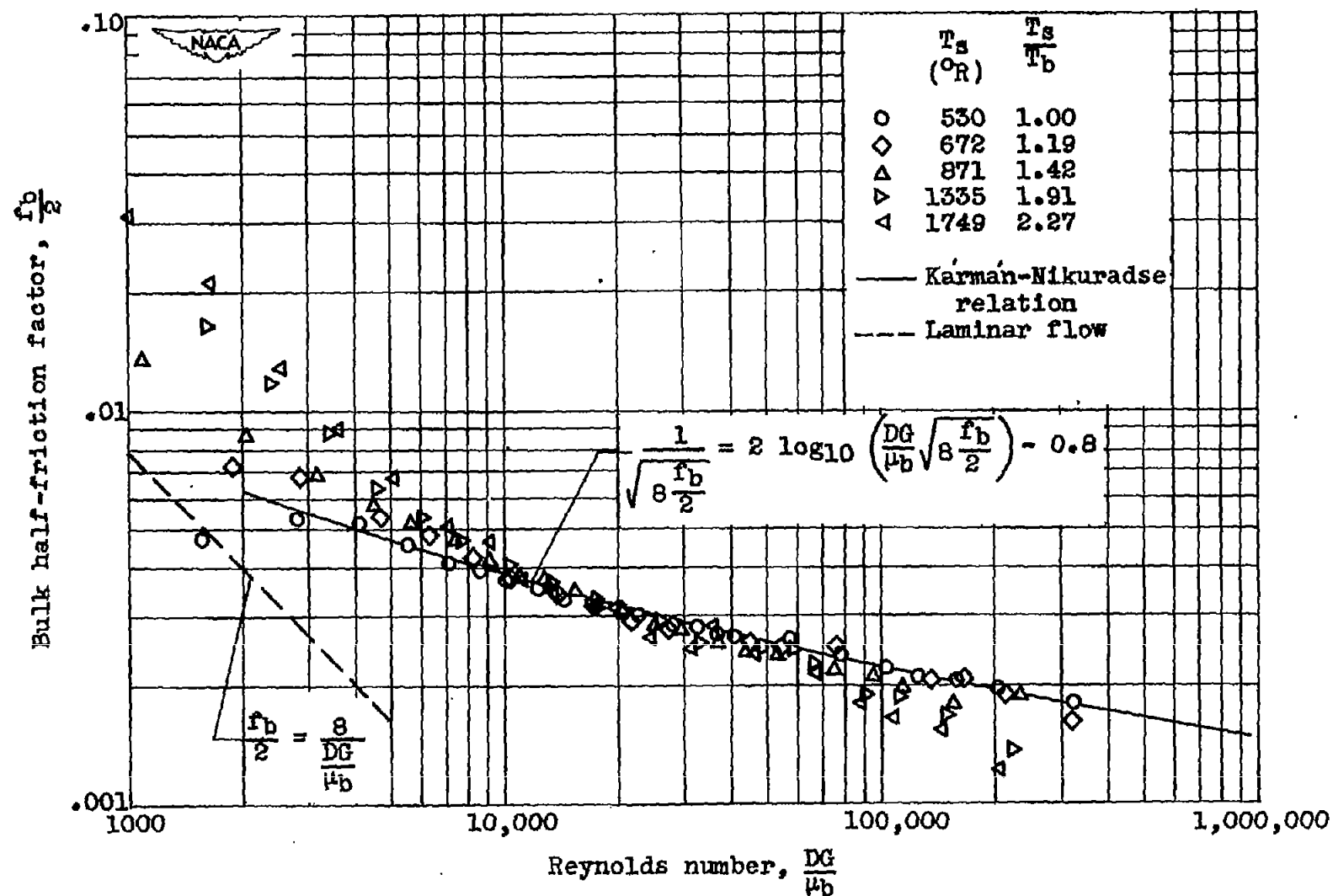


Figure 11. - Variation of bulk half-friction factor with Reynolds number with heat addition for heater tube with long-approach entrance.

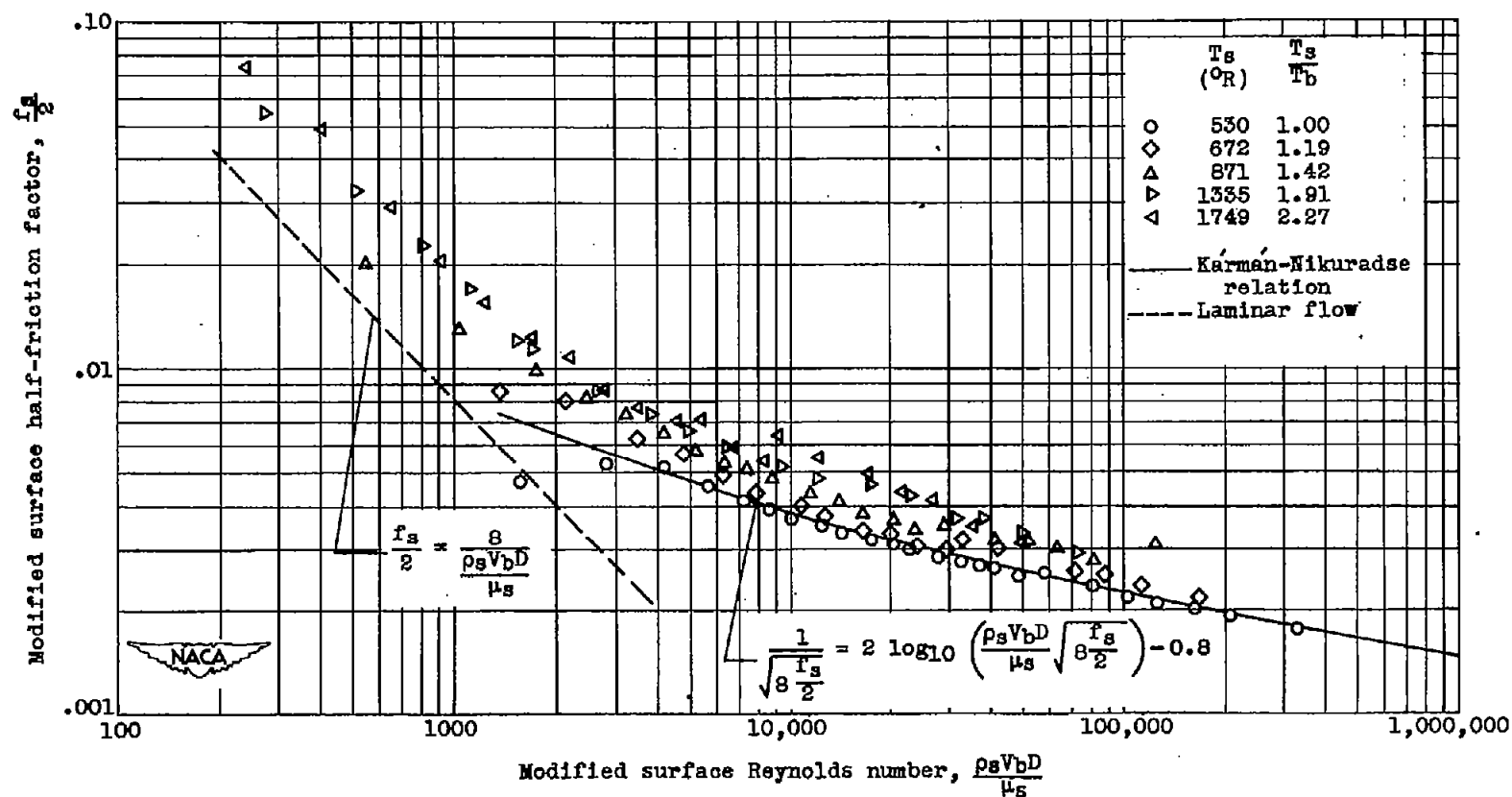


Figure 12. - Variation of modified surface half-friction factor with modified surface Reynolds number with heat addition for heater tube with long-approach entrance.

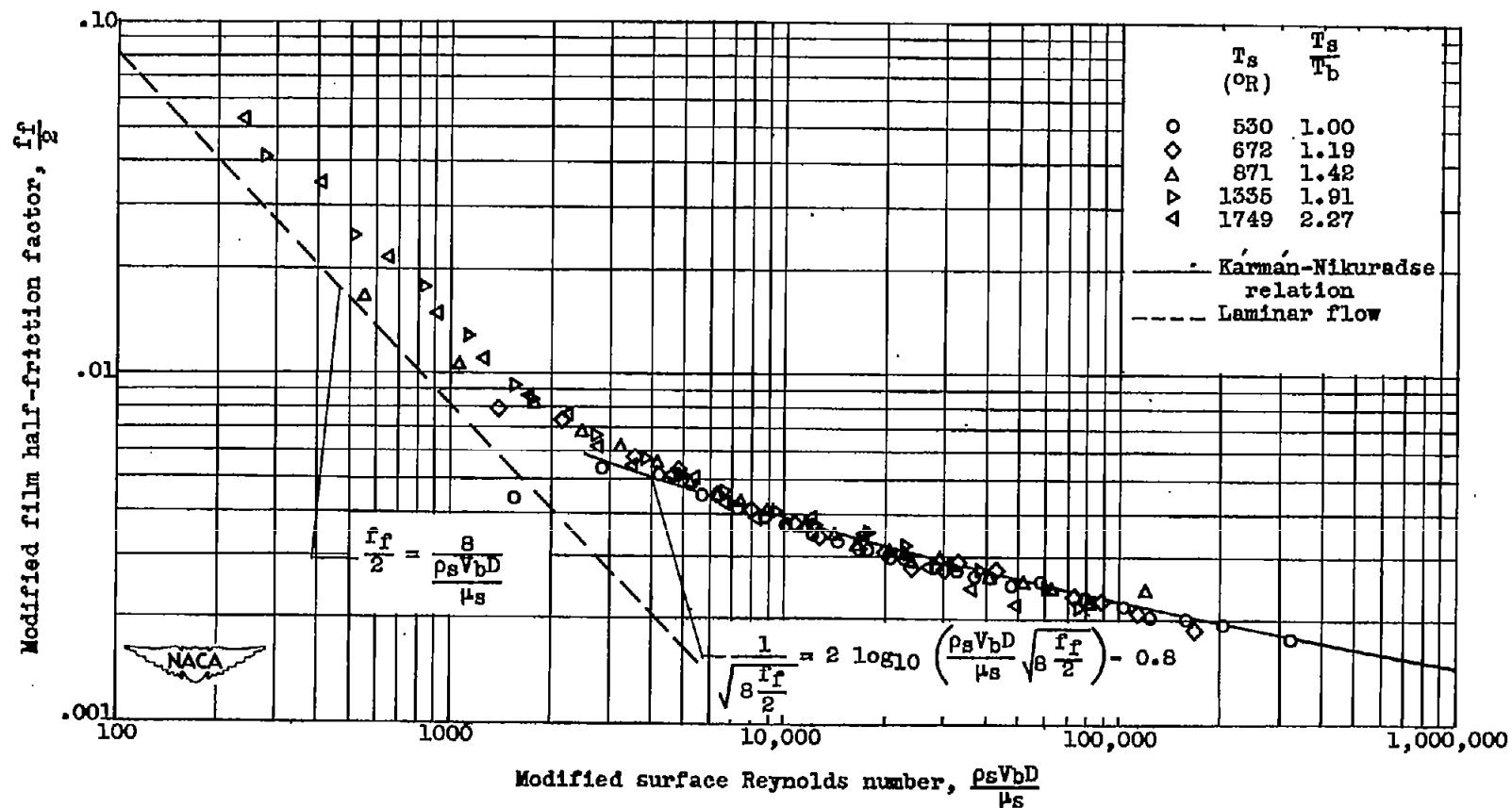


Figure 13. - Variation of modified film half-friction factor with modified surface Reynolds number with heat addition for heater tube with long-approach entrance.

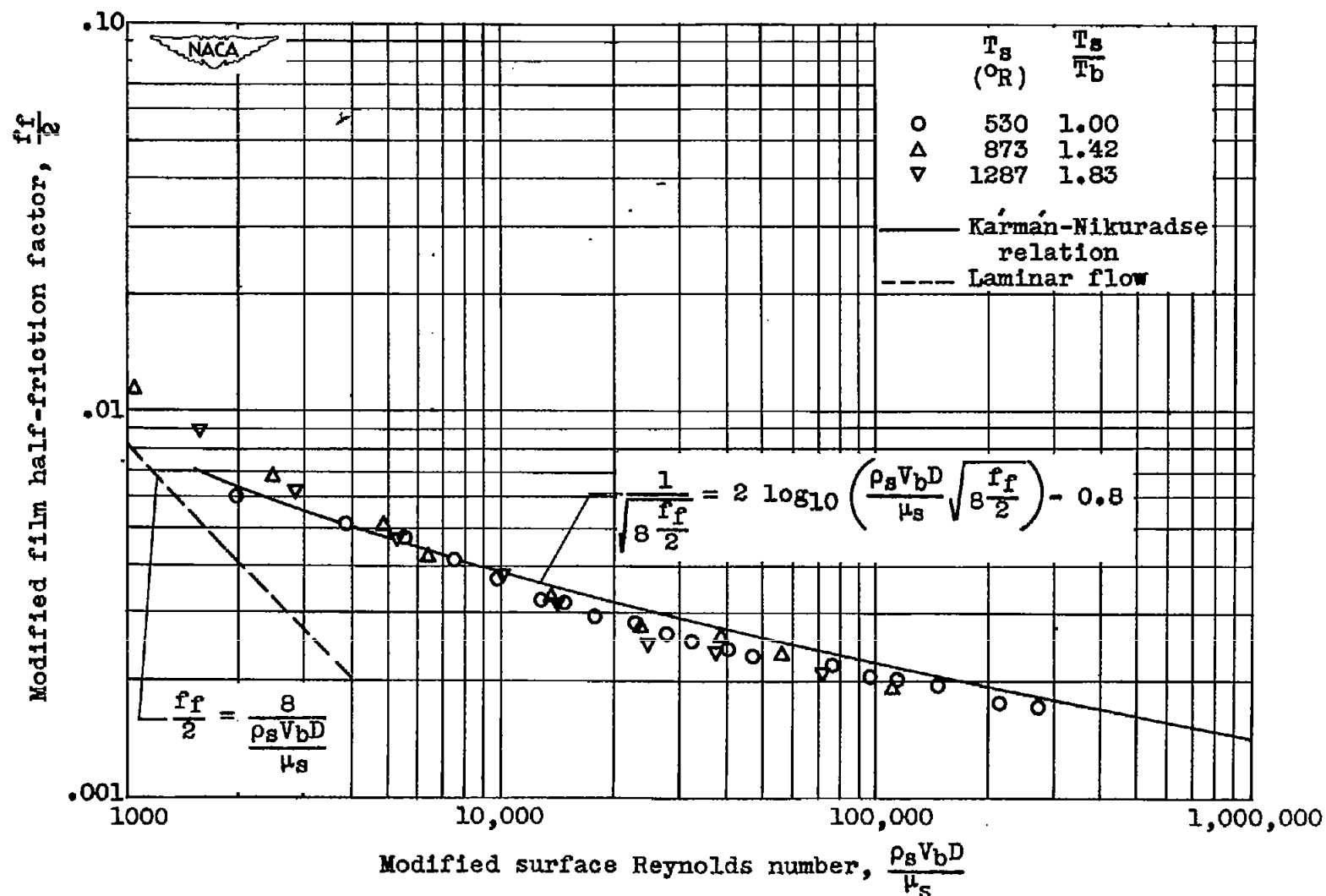


Figure 14. - Variation of modified film half-friction factor with modified surface Reynolds number with heat addition for heater tube with right-angle-edge entrance.

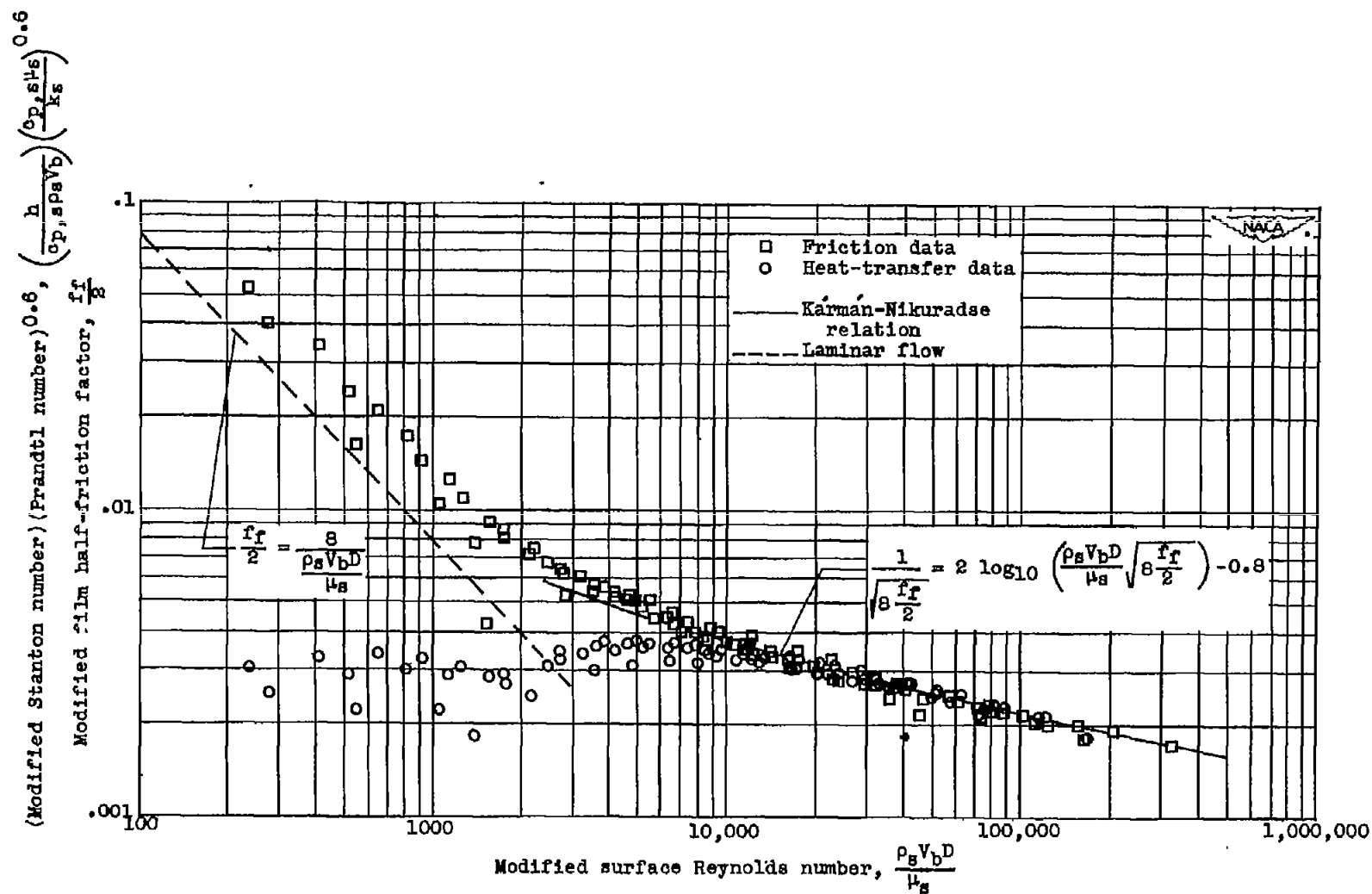


Figure 15. - Comparison of friction and heat-transfer data for heater tube with long-approach entrance.